Techno-Socio-Economic Impact of Joint Energy Resource Allocation Scheme in FiWi Network

Akshita Gupta, Vivek Ashok Bohara, and Anand Srivastava
Wirocomm Research Group, Department of Electronics & Communication Engineering,
Indraprastha Institute of Information Technology Delhi (IIITD), New Delhi, 110020, India.
Email: akshitag@iiitd.ac.in, vivek.b@iiitd.ac.in, anand@iiitd.ac.in

***Abstract*—In this paper, we consider a fiber-wireless (FiWi) network consisting of 10-Gigabit-capable passive optical network (XG-PON) and wireless fidelity (WiFi). In order to mitigate the conventional limitations of grid-power supply, an off-grid FiWi network is considered, where the components of the network such as optical network units (ONUs) and IEEE 802.11 access points (APs) are powered using renewable sources of energy such as photovoltaic (PV) panels and wind turbines along with batteries. Depending on the availability of renewable power at different locations, the energy resources available to power ONU-AP may vary. Consequently, we propose a joint energy resource allocation framework to minimize the number of PV panels and batteries required by ONU-AP based on its location as well as throughput requirement of the users. An analytical framework is derived to justify the accuracy of the proposed joint energy resource allocation framework. Further, a socio-economic analysis and trade-off analysis between allocation efficiency and cost is also presented. The results show a good agreement between the analytical and the proposed approach. It has also been observed that location with high renewable energy sources contributes to a significant reduction in the number of PV panels and batteries requirement and, therefore, has lower cost and carbon dioxide (CO_2) emissions.**

***Index Terms*—FiWi, Joint energy resource allocation, Iterative approach, Lead-acid battery, PV panel, Wind turbine, Cost-analysis, CO_2 emission.**

I. Introduction

With the increasing development and deployment of telecommunication networks, there is a demand for ubiquitous and uninterrupted connectivity. Fiber-wireless (FiWi) network consists of fiber backhaul network with wireless fronthaul. It complements the benefits of standalone wireless and optical networks to provide a network that is flexible, reliable, and has high bandwidth. In general, FiWi network has a fiber backhaul network consisting of Gigabit passive optical network (GPON) with the upstream bandwidth of 1.25 Gbps and downstream bandwidth of 2.5 Gbps [1], or 10-Gigabit-capable PON (XG-PON) with an upstream and downstream bandwidth of 2.5 Gbps and 10 Gbps [2], respectively, or 10-Gigabit-symmetric PON (XGS-PON) and next-generation PON 2 (NG-PON 2) that has 10 and 40 Gbps data rate in both the directions [3], [4], respectively. The fiber backhaul network may also constitute of IEEE 802.3ah/av 1/10 Gbps Ethernet PON (EPON) [5], [6], or next-generation Ethernet PON [7], or IEEE P802.3ca 25 Gbps EPON [8].

The wireless fronthaul network consists of various wireless standards such as, wireless fidelity (WiFi), worldwide interoperability for microwave access (WiMAX), long term evolution (LTE) 4G/ 5G radio access networks (RAN) [9]–[17]. In [9]–[11], the integration of various IEEE 802.11 standard based wireless local area network (WLAN) with XG-PON is presented. Specifically in [9] and [10], XG-PON is integrated with IEEE 802.11n and IEEE 802.11ac access points (APs), respectively to analyse the performance of dynamic bandwidth allocation algorithm for voice, video, and best-effort (BE) traffic. The authors in [12] integrated PON with wireless mesh network (WMN) to provide an energy-efficient framework for FiWi network. In [13], the authors integrated WMN with PON to study the video multicast mechanism to evaluate the quality of experience (QoE) of the users, such as video bit rate, probability of video interruption, and smoothness. An integration of PON with WiMAX as shown in [14] quantified the availability metric in IEEE P2030 standard using multi-class probabilistic availability model. Recently, a considerable literature has proposed to integrate the fiber network with RAN [15], [16]. For instance, in [16], the authors used fiber backhaul with fronthaul network with heterogeneous cloud RAN (H-CRAN) and multi-access edge computing (MEC). In [15], the authors proposed a gated service medium transparent media access control (MT-MAC) protocol for the joint optical and wireless resource management for a FiWi cloud RAN with radio antenna units operating at the millimeter-wave band. The authors integrated EPON with MEC to enhance H-CRAN and heterogeneous network (HetNet) in [16] and [17], respectively. Table I summarizes the different fronthaul and backhaul technologies used in a typical FiWi network.

II. Related works

The exponential growth in the number of devices as well as ever increasing bandwidth requirement has led to a considerable increase in the energy requirements of access networks. The energy conservation mechanisms in the existing literature usually focused on the sleeping modes of the network components to save energy, for e.g., in ITU-T G.987.3 [1], cyclic sleep and doze modes are proposed to reduce ONU power consumption for GPON. For FiWi network, researchers have tried to reduce energy consumption at both optical and wireless ends. For instance, in [18], the authors proposed energy conservation in FiWi scheme called ECO-FiWi that uses time division multiple access (TDMA) scheduling to synchronize the power-saving modes of ONU, AP, and users,

TABLE I
DIFFERENT FRONTHAUL AND BACKHAUL TECHNOLOGIES USED IN FIWI NETWORK

Reference	Technology used	Contributions
[9]	Fronthaul-XG-PON with WLAN (IEEE 802.11n)	Proposed method to enhance the quality of service for the best effort traffic.
[10]	XG-PON with WLAN (IEEE 802.11ac)	Evaluated the use of deficit dynamic bandwidth algorithm for FiWi network in order to enhance the throughput to 100 Mbps.
[11]	XG-PON with WiFi	Proposed energy resource allocation algorithm for ONU in FiWi network.
[12]	PON with wireless mesh network (WMN)	Provided a framework for an energy-efficient FiWi network by avoiding contention and frequent transmission of the packets.
[13]	PON with wireless mesh network (WMN)	Studied the video multicast mechanism to evaluate the quality of experience (QoE) of the users such as video bit rate, probability of video interruption, and smoothness.
[14]	PON with WiMAX	Quantified the availability metric in the IEEE P2030 standard using multi-class probabilistic availability model.
[16]	PON with RAN	Reduced the average delay for high-load scenarios in FiWi network with the use of optical backhaul.
[15]	PON with RAN	Proposed a gated service medium transparent MAC (MT-MAC) protocol for the joint optical and wireless resource management in FiWi network.
[16]	IEEE P802.3 ca 25 Gbps EPON with H-CRAN	Studied the resource allocation and association of users for delay-differentiated services to reduce the delay and energy consumption.
[17]	IEEE 802.3 ah or av 1 or 10 Gbps EPON with WLAN	Proposed an offloading scheme to reduce the delay and energy consumption of the network.

and use this to allocate the bandwidth to the traffic. The results showed that ECO-FiWi is able to achieve energy conservation without impacting the delay performance of the network. The authors in [19] exploited the different modes of operation for ONUs and APs to conserve energy in FiWi network. There are two modes of ONU operation, namely, sleep and active. Similarly, for AP, on and off modes are considered. The proposed energy-efficient scheme schedules the different modes of the ONU and AP and is able to achieve 73.02% of energy saving compared to the non-energy saving mechanism for a low packet arrival rate of 4,000 packets/sec and around 26.70% for a high packet arrival rate of 50,000 packets/sec. In [11], the use of solar energy for FiWi network is studied. The authors proposed resource allocation scheme for the ONU devices for on-grid as well as off-grid scenario. In [12], the authors proposed energy saving scheme for Internet of Things (IoT) over FiWi network called Adaptive Frame Aggregation with Load Transfer (AFALT). In AFALT, an adaptive frame aggregation scheme is used to analyse the channel quality of the wireless channel. Using delay-differentiated services, the priority of the voice, video, BE, and background traffic for channel access is decided. Based on the channel quality and delay, a load transfer scheme is proposed that puts the idle ONUs to sleep in order to avoid the contention. The authors were able to significantly reduce the energy consumption due to a decrease in the number of active ONUs and fewer re-transmissions of the frames due to reduced contention.

The fixed limitations of grid power, such as intermittency and large carbon dioxide (CO_2) emissions, have motivated the researchers to explore alternate sources of energy that are green and renewable. The addition of renewable energy sources will enhance the energy conservation of the network along with the reduction in carbon footprint. For instance, in [20], [21], the authors presented solar-powered base stations (BSs) for off-grid and on-grid scenarios, respectively. In [20], the authors proposed a temporal energy allocation algorithm to allocate hourly energy to the BSs, while in [21] the authors used load proportion to allocate energy to the BSs. Once the energy is allocated to the BS, the trade-off between latency and energy consumption is analysed. The authors in [22] exploited the advantages of the anti-correlated energy harvesters to use the renewable energy sources more efficiently. By deploying anti-correlated energy harvesters, the surplus power from one BS can be transferred to deficit BS. Further, the results demonstrated that with the optimization scheme, an energy conservation up to 40% can be achieved. An optimal sizing scheme for battery, photovoltaic (PV) panel, and wind-powered off-grid telecom BSs is proposed in [23]. The authors used the grey-wolf optimization method to formulate a multi-objective problem that includes the leveraged cost of electricity, excess energy, and loss of power-supply probability. The authors were able to show that with the proposed approach, they were able to get a Pareto optimal solution to the problem. However, to the best of our knowledge, a joint optimization framework to optimize the resource allocation at both wireless and optical end of FiWi network has not been investigated yet.

In addition to energy-saving, the renewable energy sources also have socio-economic impact. The economic impact of renewable energy sources such as solar power and wind turbine installed with a battery storage system is studied in [24] for a residential microgrid. In [25], the authors presented the total cost analysis for distributed and centralized energy resources for co-planning framework. The authors considered wind turbines, PV panels, and energy storage systems to analyse the total cost analysis for the transmission system. In [26] the environmental impact of the utility grid and

TABLE II
SUMMARY OF RELATED WORKS

Reference	Contributions	Remarks
[11]	Proposed energy resource allocation scheme for FiWi network	No joint energy resource allocation and no use of wind energy
[12]	Proposed AFALT scheme to minimize the energy consumption for IoT over FiWi network	No renewable energy.
[18]	Proposed ECO-FiWi scheme to conserve energy for FiWi network that schedules power saving modes of ONU, AP, and users	No renewable energy.
[19]	Exploited the different modes of operation for ONUs and APs to conserve energy in FiWi network	No renewable energy.
[20]	Proposed a temporal energy allocation algorithm to allocate hourly energy to the BSs	Use solar energy along with batteries for cellular network. No analysis for FiWi network and no use of wind power.
[21]	Used load proportion to allocate energy to the on-grid BSs	Use solar energy along with batteries for cellular network. No analysis for off-grid FiWi network and no use of wind power.
[22]	Exploited the advantages of the anti-correlated energy harvesters to power BSs	Focus on resource allocation before planning the network architecture
[23]	Proposed an optimal sizing scheme for battery, PV panel, and wind-powered off-grid telecom BSs	Includes analysis for cellular network on leveraged cost of electricity, excess energy, and loss of power supply probability. No analysis for FiWi network
[24]	Studied socio-economic impact of solar energy, wind energy and batteries on residential microgird	No joint resource allocation for FiWi network
[25]	Analysed the total cost analysis for a co-planning framework for distributed and centralized resources	No joint resource allocation for FiWi network and no social impact analysis
[26]	Analysed the CO_2 emissions for Colorado from utility grid, solar and battery powered stations	No joint resource allocation for FiWi network or cost analysis

different sources of energy such as solar energy and battery storage systems for Colorado in terms of green house gas or CO_2 emissions has been studied.

The classification of related works and their contributions are discussed in the Table II. The authors in [11] have not used wind power nor worked on joint energy resource allocation. The work proposed in [12], [18], [19] do not use any renewable sources of energy to reduce the energy consumption of FiWi network. In [20], [21], the authors used solar energy along with the batteries to allocate the energy and associate the users to the BSs. However, the authors in [20], [21] have not analysed FiWi network architecture. Moreover, they have not used wind power nor worked on joint energy resource allocation. The authors in [22], exploited the use of anti-correlated energy harvesters and to pre-plan the deployment of energy harvesters in the network. Moreover, in [23], the authors proposed an optimal sizing scheme for battery, PV panel, and wind-powered off-grid telecom BSs. However, the authors analysed the system based on leveraged cost of electricity, excess energy, and loss of power supply probability for telecom BSs but not for FiWi network. In [24], [26], the authors only worked on the cost and CO_2 analysis, respectively but not on a joint resource allocation framework for FiWi network. Similarly, the authors in [25] compared the centralized and decentralized resources but have not explored on the joint allocation framework for cellular network but not for FiWi network.

A. Contributions

Motivated by the above, this paper proposes a joint energy resource allocation framework to minimize both the batteries as well as PV panels to power the ONU-AP. The number of batteries depends on the power consumed by the ONU-AP during non-solar hours. Further, as the batteries have to be charged by the PV panels at T^{th} hour of the day, thus the number of PV panels depends on the number of batteries it has to charge. So, the number of batteries and PV panels are interdependent and therefore, they have to be jointly optimized. We have considered an off-grid FiWi network where grid supply is not available to power the FiWi network components. The off-grid networks offer several advantages such as reduce noise pollution and CO_2 emissions, the renewable sources of energy have incentives and subsidies, conventional energy systems are no longer sustainable, locations in isolated rural areas with no access to the electricity grid, the area and space available for system installation is also not an issue for most sites, increasing fuel prices because of diesel used for grid power supply, ever-growing O&M costs, they are service independence and also have cost control. However, the off-grid FiWi network has to rely on other sources of energy. The other sources can be renewable sources of energy such as solar or wind, or non-renewable sources of energy along with batteries. The renewable sources of energy are generally intermittent and may not be available to power the network component throughout the day. This increases the dependency of the FiWi network components on the battery power supply [27], [28]. Thus, energy resource allocation framework is required to allocate the energy resources based on the throughput and solar/wind power availability at the location. The co-located ONU and AP device called ONU-AP [18], [29] is powered using lead-acid batteries along with

solar and/or wind energy. A two-step iterative algorithm is proposed to minimize the number of PV panels and batteries required by ONU-AP based on location and throughput of the users connected to the network. This paper analyses the energy resource allocation framework for four different cases where ONU-APs are powered by the following sources: a) Case I: batteries with fixed PV panels, b) Case II: batteries with rotational PV panels, c) Case III: batteries with fixed PV panels and wind turbine, and d) Case IV: batteries with rotational PV panels and wind turbine. This paper considers three different locations for analysis based on their solar and wind power profile[1]. Further, in order to study the impact of network load on energy resource allocation, three kinds of average throughput requirement of the users are considered. Generally, the FiWi network consists of multiple arms, i.e., the bandwidth supplied by the OLT is splitted into multiple bandwidths at the splitter. Usually, a splitter of split ratio of 1:16 or 1:4 is considered in the literature [9], [10]. In this paper, we analyse the network performance for one arm of the network, i.e., for one ONU-AP. However, for the other arms of the network or other ONU-APs, the analysis will be similar for the other arms as evident from PON topology. The proposed framework can be easily extended and its performance can be easily evaluated. In order to capture the effect of traffic throughput distribution at different arms of the network, we consider the traffic for each node to be divided into three different categories: a) 60 Mbps, b) 40 Mbps, and c) 20 Mbps. Moreover, an analytical framework is derived to validate the accuracy of the proposed approach. In order to analyse the socio-economic impact of the energy resource allocation framework, the paper presents the economic and social impact in terms of cost and CO_2 emissions at different locations and the throughput requirement.

Some of the major contributions of the proposed work are summarized as follows:

- We propose a joint optimization framework to minimize the number of PV panels and batteries required by ONU-AP for an off-grid scenario, where ONU-AP is powered using batteries, solar power and/or wind power.
- To solve the non-linear joint optimization problem, we propose a two-step algorithm that iteratively optimize the energy resources required by ONU-AP until convergence.
- We validate the joint energy resource allocation framework for different cities across the globe based on their solar power and wind power profile.
- Additionally, we derive an analytical framework to validate the results from the iterative approach for different user throughput requirements.
- Further, we analyse the socio-economic impact of the energy resource allocation framework based on the CO_2 emission and cost analysis of FiWi network.

From the simulation results, it has been shown that the location and throughput profile plays an important role in the energy resource allocation to power ONU-AP. As the throughput increases, the power consumption of ONU-AP also increases, which increases the energy resources required by ONU-AP. Moreover, for a location with good solar/wind power, the energy resource requirement is less compared to a location with low solar/wind power. Specifically, a significant reduction of 6 PV panels and 20 batteries at 60 Mbps throughput is observed with the introduction of wind turbine and rotational PV panels for a location such as Benghazi (Libya), which has a good solar and wind power supply. While for a location with low solar supply but good wind power supply such as Moscow (Russia) has a reduction of 10 batteries and 6 PV panels with the installation of wind turbines and rotational PV panels. Similarly, a location like Jaipur (India) with good solar supply but low wind power supply has a reduction of only 7 batteries and 4 PV panels. Furthermore, the efficacy of the proposed iterative approach is validated through the derived analytical framework. In the end, the socio-economic analysis shows that there is a reduction in the cost of \$8.6/W, \$3.05/W, and \$4.61/W and a reduction in CO_2 emissions of 1.76 g/W, 0.35 g/W, and 0.98 g/W for Benghazi, Jaipur and Moscow, respectively at 40 Mbps throughput with the installation of rotational PV panels and wind turbines.

The rest of the paper is organized as follows. Section III presents the system model and parameters for the proposed FiWi network. The joint optimization problem formulation is discussed in Section IV. The proposed framework for joint energy resource allocation is presented in Section V. In Section VI, the analytical framework for the energy resource allocation algorithm is presented. Section VII contains the performance evaluation of the proposed approach. Finally, Section VIII concludes the paper.

Notations: The vector is denoted as boldface as $\mathbf{x}$. The probability density function (pdf) of the random variable is denoted as f. The set of positive real integers is denoted by $\mathbb{Z}$.

III. System Model

A. Network Model

In this paper, we consider a FiWi architecture as shown in Fig. 1. The fiber backhaul network consists of an XG-PON network[2]. The bandwidth provided by the optical line terminal (OLT) is divided among the ONUs via a passive splitter. Each ONU is connected to an AP that wirelessly provides services to the end-users. ONU and AP devices are collectively known as ONU-AP [18], [29]. The renewable energy sources are installed at ONU-AP. Precisely, it is assumed that ONU-AP is powered by different energy sources such as, PV panels, wind turbines and batteries, as shown in Fig. 2.

[1]Although the results have been obtained for three locations, the proposed analysis and energy resource allocation framework can be extended to any other locations depending on the availability of wind and solar profile data.

[2]We have use GPON because it has a higher bandwidth than EPON, thus, can provide more access to the users with better quality of service [30]. However, GPON is more complex than EPON and hence, has higher cost [30]. Moreover, for the analysis period 2020-27 GPON and EPON are projected to record a 17.9% CAGR and 16.4% CAGR, respectively [31].

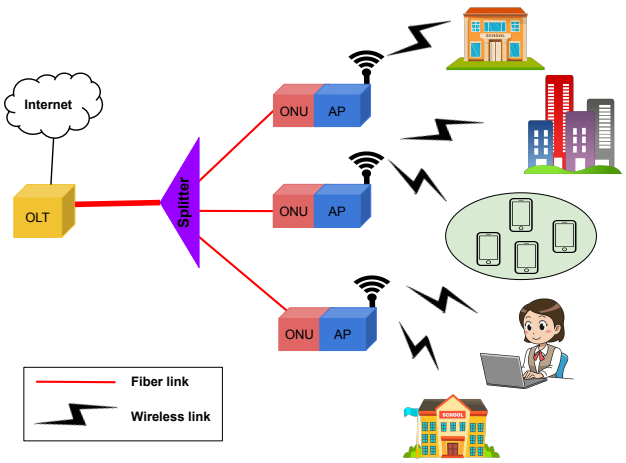

Fig. 1. FiWi network architecture.

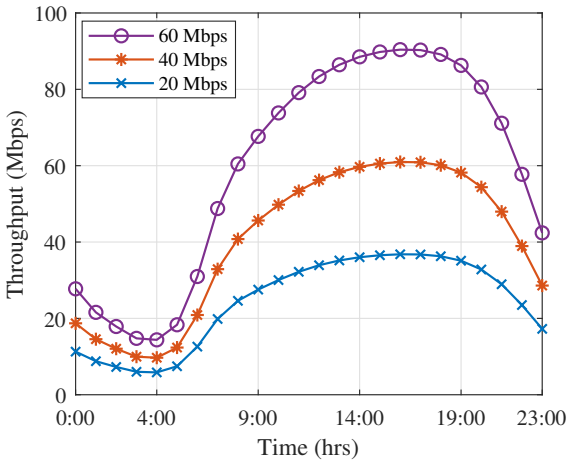

Fig. 3. Throughput profile of the users.

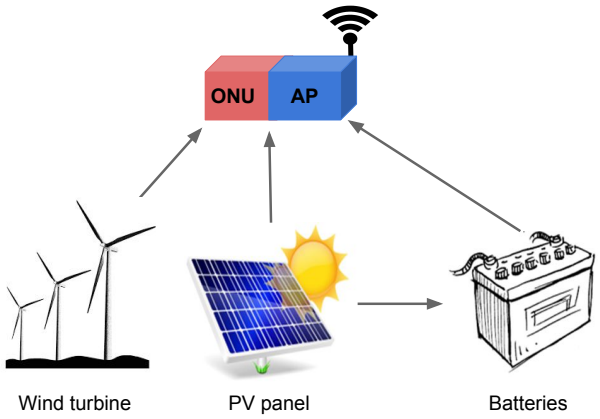

Fig. 2. System model to power ONU-AP.

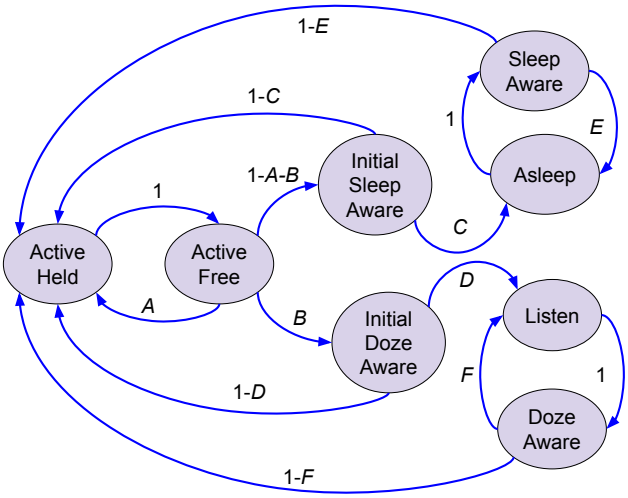

Fig. 4. State diagram for different states of ONU.

B. Traffic and Throughput Model

The density of the users connected to the network depends on the time of the day. For the peak traffic hours, the density of the users is higher as compared to the other hours. According to [32], the throughput profile for the users follows an exponential pdf given as:

$$f(y) = re^{(-ry)}, y \geq 0, \tag{1}$$

where, y is the exponentially distributed random variable, r is the rate parameter given by Gaussian mixture model (GMM) and is a function of time of the day t as [32]:

$$r = \sum_{i=1}^{k} a_i e^{\left(-\left(\frac{t-\Delta_i}{\lambda_i}\right)^2\right)}, \tag{2}$$

where, a_i is the amplitude of the i^{th} peak, Δ_i is the location of the centroid of the i^{th} peak, λ_i relates to the peak width of the i^{th} peak, t is the time (in hours) of the day, and $k = 7$ represents the number of peaks in the data series [32]. The values of $\mathbf{a} = [3.263 \times 10^6, 0.0781, 0.6616, 0.1097, 0.2584, 0.1822, 0.1652]$, $\boldsymbol{\delta} = [75.273, 3.85, 4.971, 2.996, 1.868, 3.221, -2.871]$, and $\boldsymbol{\lambda} = [12.56, 0.4829, 1.77, 0.862, 1.543, 5.972, 84]$ [32].

Fig. 3 shows the three categories of aggregate throughput profile of all the users connected to the AP [11]. It is evident that with the increase in average throughput value from 20 to 60 Mbps, the hourly throughput increases. Further, for the peak traffic hours (17:00-19:00 hrs), the number of users in the network increases, and therefore, a peak in throughput profile can be observed. Moreover, in the night (3:00-7:00 hrs), when the number of users accessing the network is low, the throughput of the network also decreases.

C. Power consumption Model

In this subsection, the power consumption profile for FiWi network devices such as ONU and AP are presented. The power consumption of the network devices depends on the throughput profile of the network. The relation between the

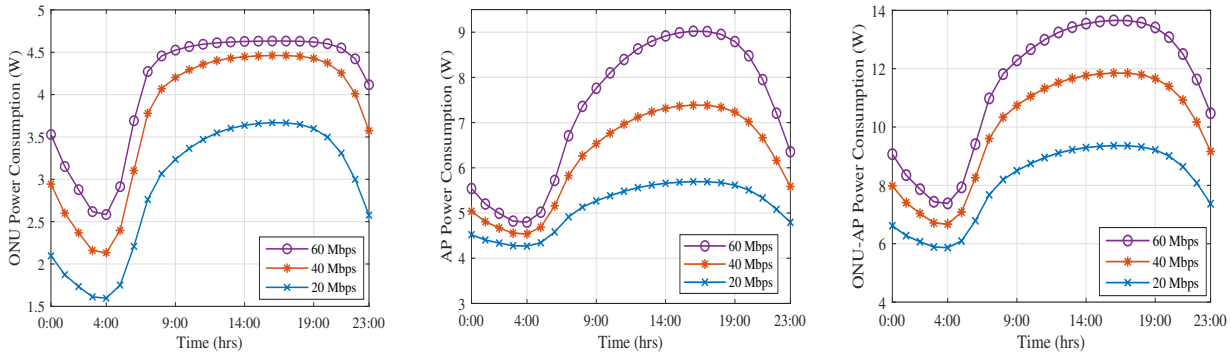

(a) (b) (c)

Fig. 5. Power consumption based on the throughput for a) ONU, b) AP, and c) ONU-AP.

power consumption and the throughput profile is described in detail below:

1) Power consumption of ONU: The power consumption of ONU depends on the various power consumption states of ONU. According to [33], the ONU can be in active held state, where ONU is awake and consumes full power, or active free state, where ONU monitors the traffic to decide whether it can go to a low power consumption state, or cyclic sleep state, where both transmitter and receiver are turned off, or doze state, where the transmitter is turned off and the receiver remains turned on or sleep aware state, where ONU checks if there was any traffic, or asleep state where transmitter and receiver are shut down, i.e., state with least power consumption. Let the power consumption of different states of ONU be denoted as sleep aware (P_{sa}), asleep (P_{as}), active held (P_{ah}), doze aware (P_{da}), listen (P_{ls}), and active free (P_{af}), then ONU's power consumption is given as [33]:

$$P_{ONU} = (\gamma_{sa_1} + \gamma_{sa_2})\, P_{sa} + \gamma_{as} P_{as} + \gamma_{ah} P_{ah} + (\gamma_{da_1} + \gamma_{da_2})\, P_{da} + \gamma_{ls} P_{ls} + \gamma_{af} P_{af}, \quad (3)$$

where, the stationary probabilities for each state is given by γ_{sa}, γ_{as}, γ_{ah}, γ_{da}, γ_{ls}, γ_{af}, respectively. Moreover, $\gamma_{sa} + \gamma_{as} + \gamma_{ah} + \gamma_{da} + \gamma_{ls} + \gamma_{af} = 1$. Each stationary probability is calculated using state transition probability as given in [33]. The transition probabilities from one state to another is given by A, B, C, D, E, and F as can be seen from Fig. 4. A represents the probability active free to active held states, B denotes the probability from active free state to doze aware state. The probability for going to asleep state from sleep aware state is given by C, D denotes the probability for going from doze aware to listen state. E denotes the probability for going from sleep aware to asleep, and F denotes the probability for going from doze aware to listen state for a discrete time Markov chain (DTMC) that represents the power management state of the ONU [33]. The distribution of transition probabilities function from one state to another is further defined in Table III [33], where δ_u and δ_d are the upstream data rate and downstream data rate, respectively. T_{sa}, T_{as}, T_{ah}, T_{da}, T_{ls}, T_{af} are the time periods of sleep aware, asleep, active held, doze aware, listen, and active free states of the ONU, respectively. In this paper, we consider symmetric data rate scenario, i.e., upstream data rate is equal to downstream data rate, i.e., $\delta_u = \delta_d$ [34], [35]. The burst size for the traffic is considered 450 bytes [11]. Fig. 5(a) shows the power consumption of the ONU with respect to the throughput profiles. It is evident that as the throughput increases, the power consumption of the ONU also increases, and the power consumption at 60 Mbps throughput is the highest, followed by 40 Mbps and 20 Mbps.

TABLE III
DISTRIBUTION OF TRANSITION PROBABILITIES [33]

Variable	Expression	Initial state	Final state
A	$1 - \exp(-\delta_u T_{af})$	Active free	Active held
B	$\exp(-\delta_d T_{af})(1 - \exp(-\delta_u T_{af}))$	Active free	Doze aware
C	$\exp(-(\delta_u + \delta_d) T_{sa})$	Asleep	Sleep aware
D	$\exp(-(\delta_u) T_{da})$	Doze aware	Listen
E	$\exp(-(\delta_u + \delta_d)(T_{sa} + T_{as}))$	Sleep aware	Asleep
F	$\exp(-(\delta_u)(T_{da} + T_{ls}))$	Doze Aware	Listen

2) Power consumption of AP: The energy consumption model for wireless IEEE 802.11 devices also depends on δ_u and δ_d. The power consumption for IEEE 802.11 APs is given as [36]:

$$P_{AP} = P_{idle} + P_{Tx} T_{Tx} + P_{Rx} T_{Rx} + \gamma_{gx} \delta_d + \gamma_{xr} \delta_u, \quad (4)$$

where, P_{idle} is the power consumption of AP in the idle mode, P_{Tx} and P_{Rx} are the transmission and reception power, respectively, T_{Rx} and T_{Tx} are the reception and transmission airtime percentage, respectively. The cross-factor for reception is denoted by γ_{xr}, i.e., processing toll per-packet in order to deliver the received frame across the protocol stack and γ_{gx} is the cross-factor of the packets generated by the application. The values of $P_{idle} = 3.68\ W$, $P_{Tx} = 0.4\ W$ and $P_{Rx} = 0.24\ W$, $\gamma_{gx} = \gamma_{xr} = 0.93 \times 10^{-3}$ [36]. The airtime percentage for the transmission and reception is also considered to be the same, i.e., $T_{Tx} = T_{Rx} = 50\%$ [37]. This is because symmetric traffic is useful as it removes

the bottleneck on the upstream traffic flow and also provide high data rate for uploading applications. There are many applications that require symmetric uplink and downlink traffic such as, content broadcast, email, file exchange, distance learning, telemedicine, online-games, etc [3]. Fig. 5(b) shows the power consumption of the AP according to the throughput. It is evident that as the network throughput increases from 20 Mbps to 60 Mbps, the power consumption of the AP also increases. Further, for the peak traffic hours the power requirement of the AP device is higher than the non-peak traffic hours.

3) Power consumption of ONU-AP: As mentioned before, the ONU and AP are collectively called ONU-AP. Thus, the power consumption of ONU-AP is the sum of the power consumption of ONU and AP device. Fig. 5(c) shows the power consumption of ONU-AP according to the different throughput requirements of the user.

D. Solar Power Model

The solar irradiance data for the solar power profile at different locations is obtained from National Renewable Energy Laboratory (NREL) [38] as well as an online repository for climate data [39]. The solar irradiance value is fed to the system advisory module (SAM) tool that converts the solar irradiance to an hourly power profile. The considered PV panels have nominal efficiency of 20.55%, an inverter of 0.01 W is used to convert DC to AC with a conversion ratio of 1.2, the inverter efficiency is 96%. The tilt of the PV panels is fixed to 30^o in the south direction. The hourly solar power profile is averaged across the year to get the 24-hour average solar profile as shown in Fig. 6. It can be seen that different regions have different solar power profiles. The 24-hour aggregated solar power for the three locations are: 45.98 W, 38.11 W, 27.34 W for Benghazi, Jaipur and Moscow, respectively[3]. Benghazi has better solar profile compared to Jaipur and Moscow. For Moscow, the solar power is available for a lesser duration of time, and the hourly power profile is also low.

E. Rotational PV panels solar power profile model

The rotation of PV panels increases the efficiency of the solar power systems. In this paper, we consider the rotational PV panels with one-time rotation per day, also known as a two-step solar tracker. Similar to two-step tracker, a concept of three-step solar tracker is mentioned in [40], where authors proposed the rotation of PV panels three times in a day corresponding to morning, noon and evening. We assume that PV panels are directed in the east-west direction, and the panels rotates from east 30^o to west 30^o at 12:00 hr. Fig. 7 shows the power profile of the PV panels with one-time rotation. The solar power profiles at different locations follow the same trend as shown in Fig. 6, but due to rotation, the duration of solar power availability as well as the power level increases.

[3]A similar analysis can be extended for other locations as well. For analysis, we have considered the locations based on solar and wind profile, i.e., Benghazi which has good solar as well as wind power, Jaipur which has good solar but low wind power and Moscow which has good wind but low solar power.

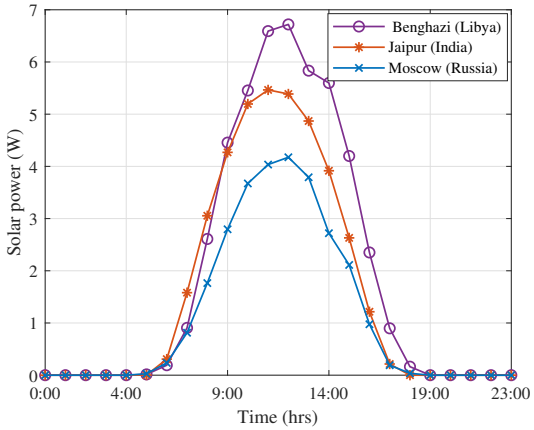

Fig. 6. Hourly solar power profiles at different locations for 10 W DC rating PV panel.

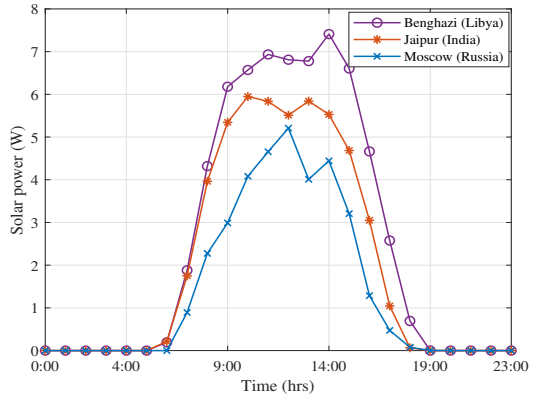

Fig. 7. Hourly solar power profiles at rotational PV panels at different locations for 10 W DC rating PV panel.

F. Wind Power Model

Wind speed depends on the height of the wind-turbine, and the location of installation. The collection of dataset for the wind speed at different locations is available in [41]. According to [41], the wind speed for Benghazi, Jaipur, and Moscow are plotted in 8(a). It is evident that the wind speed at Benghazi is the highest, whereas for Jaipur, the wind speed is the lowest. Based on the wind speed and air density (which in turn is dependent on the height of the wind-turbine), the wind power generated by the wind turbine is given by [42]:

$$P_W = 0.5\rho\pi R^2 v_w^2 C_{pmax}, \tag{5}$$

where, ρ is air density, R is blade radius of wind machine, v_w is wind speed, and C_{pmax} is the maximum rotor power coefficient. For simulations, we consider $\rho = 1.225$ kg/m^3, R =0.5 m, $C_{pmax} = 0.042$, and the height of wind turbine as 50 m. The wind power at different locations, namely,

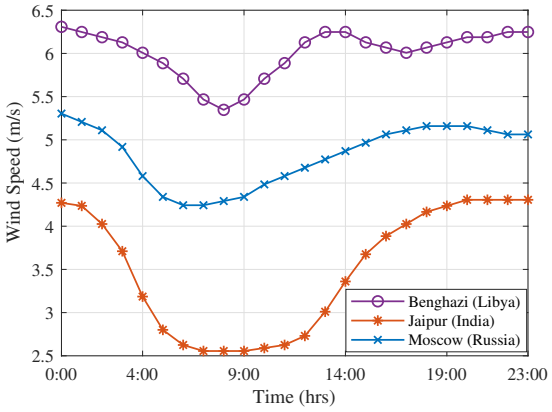

(a)

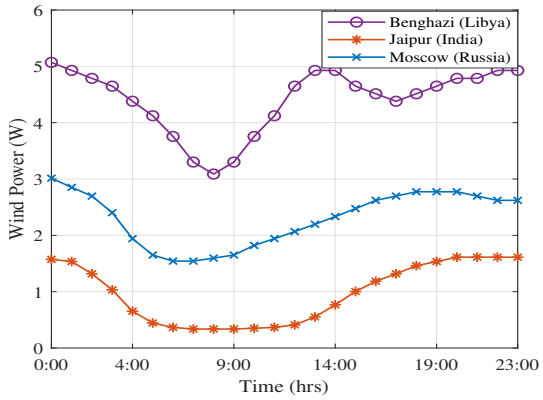

(b)

Fig. 8. a) Wind speed and b) Wind power at different locations.

Benghazi, Jaipur and Moscow is shown in Fig. 8(b). It is seen that unlike solar power, wind power is not limited to few hours in a day. For a location like Benghazi, which has high solar power profile, has high wind power profile as well. For Moscow, where the solar power profile is low, the wind power profile is higher compared to Jaipur. Furthermore, the average wind power for a day at Benghazi, Jaipur, and Moscow are 4.4126 W, 0.9721 W, and 2.3045 W, respectively. As shown in Fig. 8(b), Benghazi has the highest wind power generation potential, followed by Moscow and Jaipur. The wind power harvesting potential for Jaipur is the lowest.

G. Battery Model

One of the main energy source required to power the network components when renewable energy source is not available are the batteries. Lead-acid batteries are one of the popular types of batteries because they are cost-effective [43]. Moreover, the partial state of charge has minimal effect on the lifetime of the lead-acid batteries [43]. The batteries have a maximum charging capacity known as battery capacity (P_B^{cap}). Once the state of charge (SoC) of the batteries reaches P_B^{cap}, the batteries cannot be charged further. Moreover, whenever the batteries are discharged or charged, the SoC is updated. The operators generally specify a minimum amount of charge that must be maintained in the batteries known as dept of discharge (DoD). The battery life cycle or lifetime is enhanced if its DoD is maintained to avoid deep discharge i.e., discharge below DoD. The range of DoD is usually restricted to below 50% of the battery capacity [44]. In this paper, we have considered a series configuration of batteries, thus, if we consider a deployment scenario with N batteries of P_B^{cap} battery capacity each then, the overall capacity of the string of batteries will be NP_B^{cap} [11].

IV. Problem Formulation

A joint optimization problem where the objective is to minimize the energy resource allocated to power ONU-AP is formulated in this section. The batteries and PV panels are used to power ONU-AP, and the PV panels are also used to charge the batteries during the solar hours. It is assumed that at T^{th} hour of the day, the SoC of the battery is equal to the battery capacity.

An optimal combination of the number of batteries (N_B) and the number of PV panels (N_{PV}) needs to be calculated based on their total operational cost. Let the total operation cost for the PV panels and batteries be denoted by C_{PV} and C_B, respectively and are given as [24]:

$$C_{PV} = C_{PV}^{asset} + C_{PV}^{O\&M}, \tag{6}$$

where, C_{PV}^{asset} is the asset cost of PV panel and $C_{PV}^{O\&M}$ is the operation and management cost (O&M) of the PV panels. The total operational cost of the batteries is given as [24]:

$$C_B = C_B^{asset} + C_B^{O\&M} + N_B^{rep} C_B^{asset}, \tag{7}$$

where, C_B^{asset} is the asset cost of the battery, $C_B^{O\&M}$ is the O&M cost of the battery, and N_B^{rep} is the number of times the batteries are needed to be replaced during the lifetime of the system.

In this paper, all the analysis is done on hourly basis, i.e. for $t \in [0, 23]$ hour. The hourly solar power profile for single PV panel is given by $P_S^1(t), \forall\ t \in [0, 23]$. Similarly, the state of charge of a single battery is denoted by $P_{SoC}^1(t), \forall\ t \in [0, 23]$. The DoD limit for each battery is denoted by βP_B^{cap}. Consequently, the hourly power consumption of ONU-AP is defined by $P_{ONU-AP}(t), \forall\ t \in [0, 23]$.

The optimization problem thus formulated is given as:

$$(P1) \min_{N_{PV}, N_B} N_{PV} C_{PV} + N_B C_B, \tag{8}$$

$$s.t.\ \beta P_B^{cap} \leq P_{SoC}^1(t) \leq P_B^{cap},\ \forall\ t \in [0, 23], \tag{9}$$

$$P_{SoC}^1(T) \geq P_B^{cap}, \tag{10}$$

$$N_{PV} P_S^1(t) + N_B P_{SoC}^1(t) \geq P_{ONU-AP}(t),\ \forall\ t \in [0, 23]. \tag{11}$$

Here, (8) represents the optimization function to minimize the overall cost of the system, where, $N_B, N_{PV} \in \mathbb{Z}$. The first constraint in (9), is used to maintain the charge in the battery between βP_B^{cap} and P_B^{cap}. The second constraint in (10) denotes that each battery must be entirely charged at T^{th} hour of the day. The third constraint in (11) represents that for each

hour, the power from N_B batteries and N_{PV} PV panels must be able to fulfill the power demand of ONU-AP.

It should be noted that (8) is a linear integer objective function, where, the optimization variables $N_{PV}, N_B \in \mathbb{Z}$. However, due to the last constraint in (11) which is quadratic in nature, the optimization problem is a quadratic constraint linear programming problem (QCLP) [45], which is a special case of quadratic constraint quadratic programming (QCQP) [46]. In order to find an optimal solution for problem $(P1)$, the quadratic constraint in (11) could be converted to separable variables as discussed in [47]. However, even if the last constraint in (11) is converted to separable variable form, the problem is still non-linear and the Hessian matrix will have positive and negative eigenvalues. Thus, the problem will not have any global maximum or minimum. Therefore, in order to solve this problem, we propose a two-step iterative approach [45], which is discussed in detail in Section V.

V. Proposed Method for Joint Energy Resource Allocation

In this section, we describe the two-step iterative algorithm to get a solution for the non-convex problem. First, we present the algorithm for minimizing the number of batteries required by ONU-AP. Later, we present the algorithm for minimizing the number of PV panels required to power ONU-AP and charge the batteries required by ONU-AP. Finally, we present an iterative algorithm to converge the number of PV panels and batteries needed by ONU-AP[4].

A. Algorithm to calculate minimum number of batteries

In this subsection, the algorithm to calculate minimum number of batteries required by the ONU-AP is presented. As the paper considers an off-grid environment, the batteries are used to power ONU-APs when solar power is unavailable. The Algorithm 1, considers a heuristic method where the battery power changes for each loop. Considering that at each iteration of the loop the total battery capacity, P_B^{cap} increases in the multiple of single battery capacity P_B^{cap}.

As discussed earlier, the batteries should be charged by the PV panel at T^{th} hour. Therefore, we initialize the battery power at T^{th} hour, $P_B(T) = P_B^{cap}$. For each hour t, the power is drawn from the PV panel, $P_S(t)$ is calculated as:

$$P_S(t) = \min\left\{P_{ONU-AP}(t), P_S^M(t)\right\}, \tag{12}$$

where, $P_S^M(t)$ is the power of the PV panel at time t. Now, we check whether the power from PV panels is sufficient to charge to ONU-AP:

$$P_{ONU-AP}(t) - P_S^M(t) = \begin{cases} \leq 0, & \text{if the power is sufficient} \\ > 0, & \text{if the power is deficit} \end{cases} \tag{13}$$

[4]The energy resource allocation for FiWi network consisting of XG-PON and WLAN is proposed in this paper. However, the change of technology from GPON to EPON or WLAN to other wireless technology, such as WiMAX or WMN, would not alter the operation of the proposed algorithm. The proposed algorithm is agnostic to FiWi framework employed.

In case the power from the PV panel is not sufficient, the deficit power supplied by the batteries is given as:

$$P_{def}(t) = P_{ONU-AP}(t) - P_S(t), \tag{14}$$

otherwise, $P_{def}(t) = 0$. Similarly, in cases where power from PV panels is not sufficient to power ONU-AP, there will be no excess power available with the PV panel, $P_S^{ex} = 0$. Otherwise, the excess power from the PV panel is given as follows:

$$P_S^{ex} = P_S^M(t) - P_S(t). \tag{15}$$

In order to satisfy the constraint in (9), the power of each battery at each hour t, must be in between βP_B^{cap} and P_B^{cap}. Thus, it is necessary that the power in the battery allocated for the next hour of operation $P_{SoC}(t+1) = P_{SoC}(t) - P_{def}(t) + P_S^{ex}(t)$ is not below $\beta P_B^{cap,N}$ or more than $P_B^{cap,N}$. Therefore, the number of times in a day the battery power is going below $\beta P_B^{cap,N}$ is counted using a variable $P_o(t)$, which is 1 every time the battery power is below $\beta P_B^{cap,N}$. The algorithm stops once, B_{cap} is enough to satisfy that the battery does not discharge beyond $\beta P_B^{cap,N}$ at any time t. Algorithm 1 presents the algorithm to calculate the minimum number of

Algorithm 1 The battery allocation algorithm

Input:
$Count_{PV}$ = Number of PV panels
Initialize:
$P_{SoC}(T) = P_B^{cap}$
$P_o = 1 \times 24$ vector with all values = 1
$Count_B = 1$
$P_S^M = Count_{PV} \times P_S^1$

while $\sum_{t=0}^{23} P_o(t) = 0$ **do**
  for $t = T$ to $T + 23$ **do**
    $P_B^{cap,N} = Count_B \times P_B^{cap}$
    $P_S(t) = \min\{P_{ONU-AP}(t), P_S^M(t)\}$
    if $P_{ONU-AP}(t) - P_S(t) > 0$ **then**
      $P_{def}(t) = P_{ONU-AP}(t) - P_S(t)$
      $P_S^{ex}(t) = 0$
    else
      $P_{def}(t) = 0$
      $P_S^{ex}(t) = P_S^M(t) - P_S(t)$
    end if
    if $P_{SoC}(t+1) - P_{def}(t) + P_S^{ex}(t) < \beta P_B^{cap,N}$ **then**
      $P_o(t) = 1$
    else
      $P_o(t) = 0$
    end if
    $P_{SoC}(t+1) =$
    $\min\{P_{SoC}(t) - P_{def}(t) + P_S^{ex}(t), P_B^{cap,N}\}$
  end for
  $Count_B = Count_B + 1$
end while

Output: The value of $Count_B$ is the minimum batteries required by ONU-AP for $Count_{PV}$ PV panels.

batteries required by ONU-APs without any deep discharge. The complexity of Algorithm 1 is calculated as $\mathcal{O}(Count_B)$.

Algorithm 2 The PV panel allocation algorithm

Input:
$Count_B$ = Number of batteries
Initialize:
$P^N_{SoC}(T) = Count_B \times P^{cap}_B$
$P_o = 1 \times 24$ vector with all values = 1
$Count_{PV} = 1$
$P^{cap,N}_B = Count_B \times P^{cap}_B$

while $P_{SoC}(T+24) = P^{cap,N}_B$ **do**
  for $t = T$ to $T+23$ **do**
    $P^M_S(t) = Count_{PV} \times P^1_S(t)$
    $P_S(t) = \min\{P_{ONU-AP}(t), P^M_S(t)\}$
    if $P_{ONU-AP}(t) - P_S(t) > 0$ **then**
      $P_{def}(t) = P_{ONU-AP}(t) - P_S(t)$
      $P^{ex}_S(t) = 0$
      $P_{min} = \min\{P_{SoC}(t) - P_{def}(t) + P^{ex}_S(t), P^{cap,N}_B\}$
      $P^N_{SoC}(t+1) = \max\{P_{min}, \beta P^{cap,N}_B\}$
    else
      $P_{def}(t) = 0$
      $P^{ex}_S(t) = SP(t) - P_S(t)$
      $P_{min} = \min\{P^N_{SoC}(t) - P_{def}(t) + P^{ex}_S(t), P^{cap,N}_B\}$
      $P^N_{SoC}(t+1) = \max\{P_{min}, \beta P^{cap,N}_B\}$
    end if
  end for
  $Count_{PV} = Count_{PV} + 1$
end while

Output: The value of $Count_{PV}$ is the minimum PV panels required by ONU-AP for $Count_B$ batteries.

B. Algorithm to calculate minimum number of PV panels

As we consider an off-grid scenario thus, the batteries can only be charged by the PV panels. The PV panels are used to power ONU-AP as well as charge the batteries for operation during non-solar hours. To calculate the minimum number of PV panels required by ONU-AP, we propose Algorithm 2, as discussed below. The batteries must be completely charged at T^{th} hour, for this, consider the power supplied by the PV panel to ONU-AP given as:

$$P_S(t) = \min\left\{P_{ONU-AP}(t), P^M_S(t)\right\}. \tag{16}$$

If the power supplied by the PV panels is not enough to fulfill the power demand of ONU-AP, the power needs to be extracted from the batteries. The deficit power supplied by the batteries is given as:

$$P_{def}(t) = \begin{cases} 0, & \text{if } P_{ONU-AP}(t) - P_S(t) \leq 0 \\ P_{ONU-AP}(t) - P_S(t), & \text{otherwise.} \end{cases} \tag{17}$$

Further, in order to satisfy constraint in (9), we need to check the battery state at the beginning of the next hour. The battery state, $P_{SoC}(t+1)$ must be between $\beta P^{cap,N}_B$ and $P^{cap,N}_B$. The battery power state at the beginning of the next hour $P^N_{SoC}(t+1)$ is given as follows:

$$P_{min} = \min\{P^N_{SoC}(t) - P_{def}(t) + P^{ex}_S(t), P^{cap,N}_B\}, \tag{18}$$

$$P^N_{SoC}(t+1) = \max\{P_{min}, \beta P^{cap,N}_B\}. \tag{19}$$

The constraint in (10) must be met in order to entirely charge the batteries at the beginning of next T^{th} hour:

$$P^N_{SoC}(T+24) = P^{cap,N}_B. \tag{20}$$

The number of PV panels for which (20) is met, gives the minimum number of PV panels required by the system. Similar to Algorithm 1, the complexity of Algorithm 2 is: $\mathcal{O}(Count_{PV})$.

C. Iterative approach

The iterative algorithm for solving the optimization problem (8) is based on a two-way iteration between minimum batteries and minimum PV panels and is described concisely in Algorithm 3 [48]. Initially, we fix the number of batteries to N_B (Here, we have initialized the algorithm with fixed number of batteries, however, we could also initiate with fixed number of PV panels). For N_B batteries, we calculate the minimum number of PV panels required to power the ONU-AP. For the calculated number of PV panels, we calculate the minimum number of batteries. This process goes on until converges is obtained, i.e., number of batteries and PV panels calculated from the current iteration, $(k+1)^{th}$ is equal to the number of batteries and PV panels of previous iteration, i.e., k^{th} iteration. For Algorithm 3, the iterative approach iterates Algorithm 1 and Algorithm 2 until convergence. Thus, the complexity of Algorithm 3 is: $\mathcal{O}(k(Count_B + Count_{PV}))$, where k denotes the number of iterations after which the algorithm converges.

Algorithm 3 The iterative algorithm

Initialize: The number of batteries, N_B to a random integer

1: Calculate the minimum number of PV panels (N_{PV}) required to power ONU-AP and charge the N_B batteries at the T^{th} hour
   - N_{PV} = The PV panel allocation algorithm (N_B)
2: Calculate the minimum number of batteries required (N_B) to power ONU-AP given N_{PV} PV panels
   - N_B = The battery allocation algorithm (N_{PV})
3: Go back to step 1 and iterate until convergence.

VI. Analytical framework

The power in the batteries must be able to fulfill the demand of ONU-AP during non-solar hours, P^{ONU-AP}_{NS}. Considering the battery capacity of a single battery as P^{cap}_B, the power available by the batteries to charge ONU-AP is given by $P^{cap}_B - \beta P^{cap}_B$. Therefore, the number of batteries required by ONU-AP, N_B is given as:

$$N_B(P^{cap}_B - \beta P^{cap}_B) = P^{ONU-AP}_{NS}, \tag{21}$$

TABLE IV
DURATION OF SOLAR POWER PROFILE AVAILABLE TO POWER ONU-AP

	Case I: Batteries + fixed PV panels	Case II: Batteries + rotational PV panels	Case III: Batteries + fixed PV panels + wind turbine	Case IV: Batteries + rotational PV panels + wind turbine
Benghazi	6:45 to 17:00	6:45 to 18:00	7:00 to 17:45	7:00 to 17:45
Jaipur	6:45 to 17:15	6:45 to 17:30	6:45 to 17:15	6:45 to 17:15
Moscow	6:45 to 17:00	6:45 to 17:15	6:45 to 17:00	6:45 to 17:15

$$N_B = \frac{P_{NS}^{ONU-AP}}{(P_B^{cap} - \beta P_B^{cap})}, \tag{22}$$

$$N_B = \frac{P_{NS}^{ONU-AP}}{(1-\beta) P_B^{cap}}. \tag{23}$$

The PV panel power available to the batteries is given as:

$$P_{PV}^{Bat} = \sum_{i=0}^{23} P_S^M(i) - P_S^{ONU-AP}, \tag{24}$$

where, P_S^{ONU-AP} is the power of PV panel consumed during solar hours and P_S^M is the hourly solar power profile of N_{PV} PV panels. (25) can be rewritten as:

$$P_{PV}^{Bat} = N_{PV} \sum_{i=0}^{23} P_S^1(i) - P_S^{ONU-AP}, \tag{25}$$

where, N_{PV} be the minimum number of PV panels required by ONU-AP and P_S^1 is the hourly solar power profile of a single PV panel.

It is well known fact that PV panel power can be used to charge the batteries. Thus, the power of the PV panels available to the batteries must be equal to the power available by the batteries to charge the ONU-AP, i.e.:

$$P_{PV}^{Bat} - N_B(P_B^{cap} - \beta P_B^{cap}) = 0, \tag{26}$$

$$P_{PV}^{Bat} = N_B(P_B^{cap} - \beta P_B^{cap}). \tag{27}$$

Using (25), (27) can be written as:

$$N_{PV} \sum_{i=0}^{23} P_S^1(i) - P_S^{ONU-AP} = N_B(P_B^{cap} - \beta P_B^{cap}), \tag{28}$$

$$N_{PV} = \frac{N_B(P_B^{cap} - \beta P_B^{cap}) + P_S^{ONU-AP}}{\sum_{i=0}^{23} P_S^1(i)}. \tag{29}$$

Depending on the locations, the duration of solar power supplied to ONU-AP also varies. Table IV summarizes the considered duration of solar power availability to fulfill the demand of ONU-AP. For instance, Benghazi has a good solar profile, thus, the duration for which the PV panels can supply power to ONU-AP is also longer, while for the location such as Moscow, the solar power supplied to ONU-AP is for a short duration. Similarly, with rotational PV panels, the duration of solar power profile available to power ONU-AP is higher compared to fixed PV panels. An increase in one hour solar power duration for Benghazi can be observed from Table IV due to rotational PV panels. Furthermore, with the introduction of wind power, the effective power consumed by ONU-AP from PV panels and batteries reduces, thus PV panel might be able to charge ONU-AP even during the low solar power hours and the effective duration for which PV panels can supply power to the ONU-AP increases. For instance, an increase of 30 min solar power duration for Benghazi because of high wind power, but at Jaipur and Moscow there is no increase in the duration of solar power supply as the wind power at Jaipur and Moscow is low. Similarly, it is interesting to observe that with the installation of both the wind turbines and rotational PV panels, the duration for which solar power supply is available to power ONU-AP further increases.

VII. PERFORMANCE EVALUATION

In this section, the performance of the iterative and analytical approach to minimize the energy resources required to power ONU-AP is discussed. The energy resource allocation scheme for four different cases are compared: a) Case I: Batteries with fixed PV panels, b) Case II: Batteries with rotational PV panels, c) Case III: Batteries with fixed PV panels and wind turbine, and d) Case IV: Batteries with rotational PV panels and wind turbine. For wind power, we consider a wind turbine with parameters specified in Section II. The capacity of the single battery is considered to be 5W [49]. The DC power rating of a single PV panel is 5W [50]. Moreover, for analysis, we consider that at time T = 16:00 hrs the PV panels entirely charge the batteries. The DoD value for the battery, β is considered 0.7 [21].

A. Iterative and Analytical approach

This subsection presents the results for the iterative approach and compares the results from the algorithm with the analytical framework proposed in Section V.

Fig. 9 shows the minimum number of PV panels and batteries required to power an ONU-AP for case I when the batteries and fixed PV panels are installed to power ONU-AP. Considering the assumptions mentioned in Table IV, it can be observed that the theoretical values for the number of PV panels and batteries is in agreement with the results from the two-way iterative approach. Moreover, as the throughput increases, the number of PV panels and batteries required by ONU-AP also increases. This is because, with the increase in throughput, the power consumption of ONU-AP increases, therefore, more batteries and PV panels are required by ONU-AP. Further, it can be observed that for Benghazi, where the solar power profile is higher compared to Jaipur and Moscow, the number of PV panels and batteries required by ONU-AP is less compared to other cities. For instance, for 20 Mbps

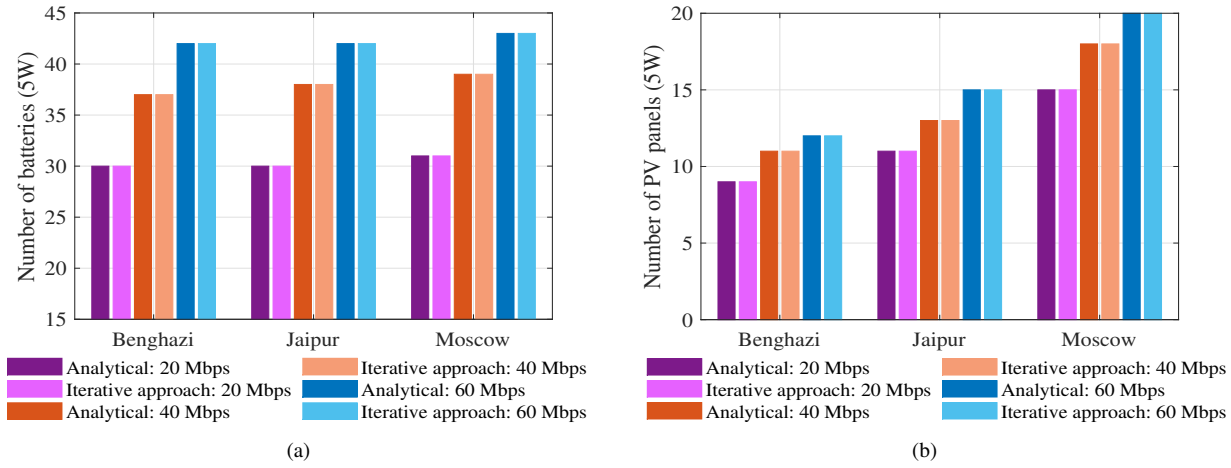

Fig. 9. Minimum a) Number of batteries and b) Number of PV panels for Case1: Batteries with fixed PV panels.

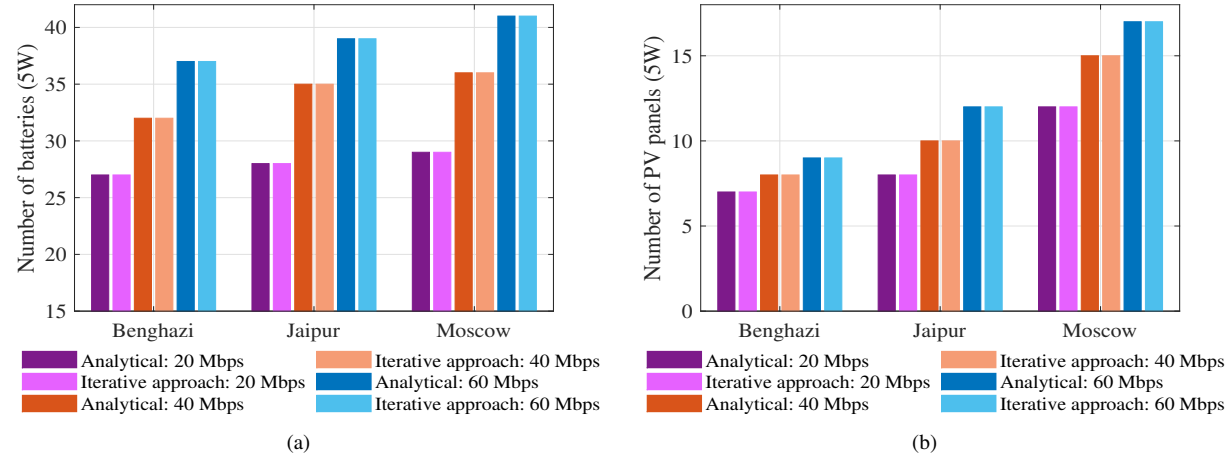

Fig. 10. Minimum a) Number of batteries and b) Number of PV panels for Case II: Batteries with rotational PV panels.

throughput, the number of PV panels and batteries required at Benghazi are 30 and 9, respectively, whereas the number of PV panels and batteries required at Moscow increases to 31 and 15, respectively.

Fig. 10 presents the minimum number of PV panels and batteries required to power ONU-AP for case II, i.e. when the batteries with rotation PV panels are installed to power ONU-AP. The analytical values are in consensus with the proposed algorithm results, verifying the accuracy of the iterative approach. Further, it is evident that with the increase in throughput, the number of PV panels and batteries required by ONU-AP also increases. For instance, an increase of 10 batteries and 2 PV panels can be observed as the throughput increases from 20 Mbps to 60 Mbps at Benghazi. Further, a clear impact on the allocation of energy resources can be seen as the location of installation changes from higher solar profile location to lower solar profile location. Moreover, compared to Fig. 9, utilizing rotation of PV panels reduces the number of batteries from 30 to 27 at Benghazi for 20 Mbps throughput, and the number of PV panels are reduced from 9 to 7.

Fig. 11 shows the impact of the installation of wind turbines with fixed PV panels and batteries for analytical and iterative approach. The results for iterative approach are in agreement with the analytical results. Compared to case I, the number of PV panels and batteries is reduced significantly. As the wind power is not limited to a certain number of hours in a day thus, the effective power requirement of ONU-AP consumed via batteries and PV panels reduces, and with the reduction in power consumption of ONU-AP, the energy resource allocation also reduces. The number of batteries reduces from 30 to 12 at Benghazi for 20 Mbps throughput with the introduction of wind turbines. Similarly, a reduction of 5 PV panels can be observed with the installation of wind turbines. It can be observed that the wind power for Benghazi is the highest; thus, a saving of >50% of the batteries and PV panels can be seen compared to case I, while, for Jaipur, there

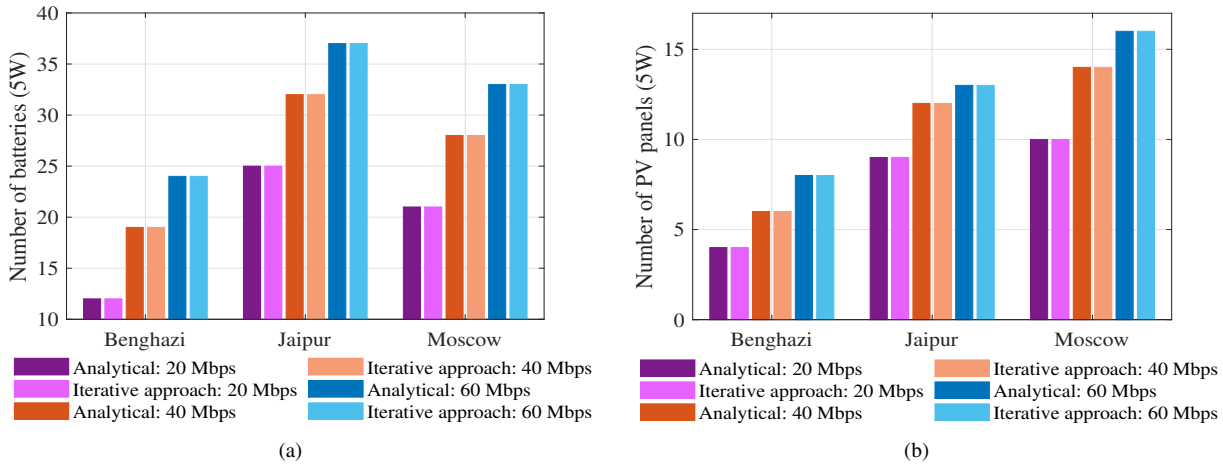

Fig. 11. Minimum a) Number of batteries and b) Number of PV panels for Case III: Batteries with fixed PV panels and wind turbine.

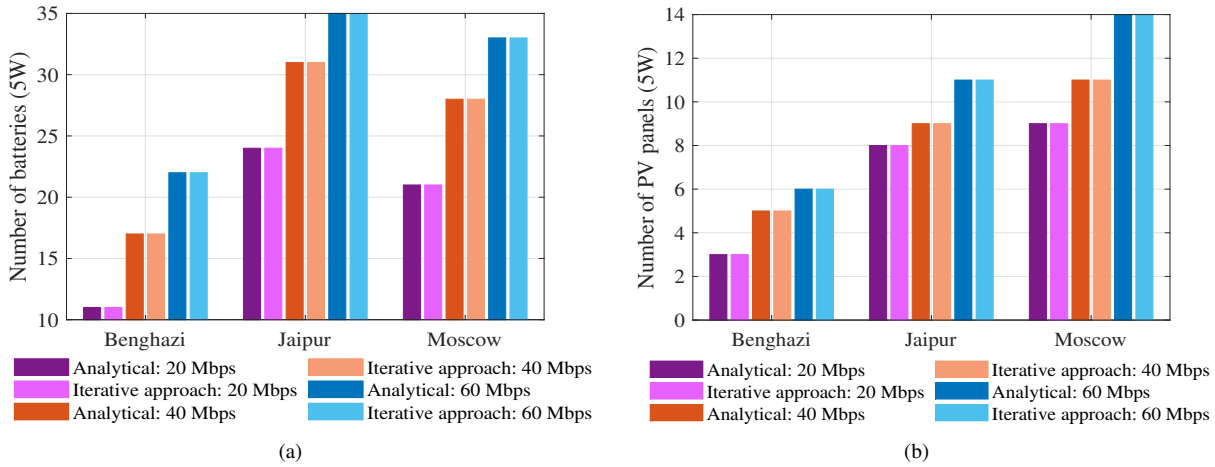

Fig. 12. Minimum a) Number of batteries and b) Number of PV panels for Case IV: Batteries with rotational PV panels and wind turbine.

TABLE V
COST AND CO_2 EMISSION ANALYSIS OF BATTERIES AND PV PANELS

	Battery	PV panel	Wind turbine
Cost ($/W)	20.562	4.20	3.520
CO_2 emissions (g/W) [26]	4.22	0.96	0.96

is only a saving of 5-6 batteries and 1-2 PV panels because wind power is the lowest for Jaipur, and for Moscow, there is a reduction of 8 batteries and 3-4 PV panels. Thus, it can be inferred that the reduction in the energy resource requirement is proportional to the amount of wind power harvested at the location. For case IV, where batteries along with rotational PV panels and wind turbine are installed at ONU-AP, the number of PV panels and batteries reduces further as can be seen from Fig. 12. Further, it can be seen that the number of batteries reduces from 42 to 22, and the number of PV panels reduces from 12 to 6 for case IV compared to case I at Benghazi for 60 Mbps throughput. Moreover, compared to case II, there is a reduction of 15 batteries and 3 PV panels for 60 Mbps throughput at Benghazi.

B. Cost analysis

In this subsection, we evaluate the cost analysis of the resource required to power the ONU-AP. The cost for batteries and PV panels are calculated using (7) and (30), respectively. The asset cost of the batteries $C_B^{asset} = \$195/kWh = \$4.680/W$ for a day, the O&M cost of the batteries are, $C_B^{O\&M} = 2\%$ of C_B^{asset} [24][5], the lifetime of the batteries is assumed to be 5 yrs [11], thus for a system lifetime of 20 yrs, there is a need to replace the batteries three times, therefore, $N_B^{rep} = 3$, the asset cost for the PV panels and wind turbines are $C_{PV}^{asset} = \$3000/kWh = \$72/W$ for a day and $C_W^{asset} = \$2500/kWh = \$60/W$ for a day, respectively

[5]However, these cost might vary depending on the country. For this paper, we have used the cost given in [24].

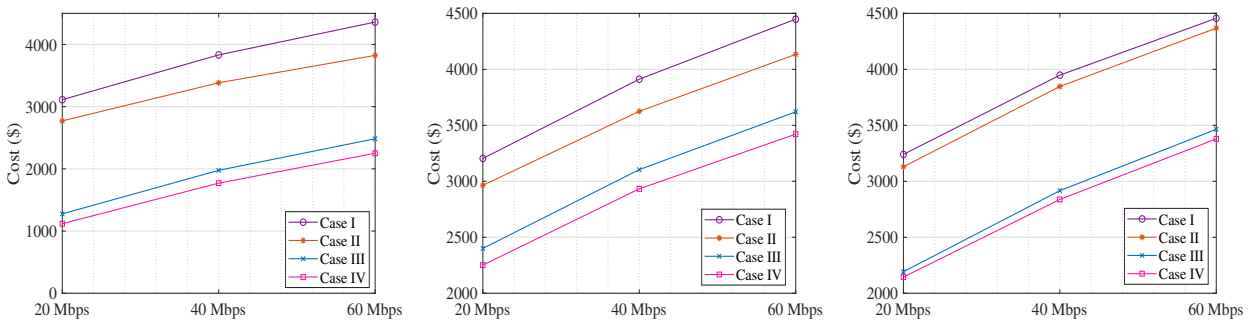

Fig. 13. Cost analysis for a) Benghazi, b) Jaipur, and c) Moscow for Case I: Batteries with fixed PV panels, Case II: Batteries with fixed PV panels, Case III: Batteries with fixed PV panels and wind turbine, and Case IV: Batteries with rotational PV panels and wind turbine.

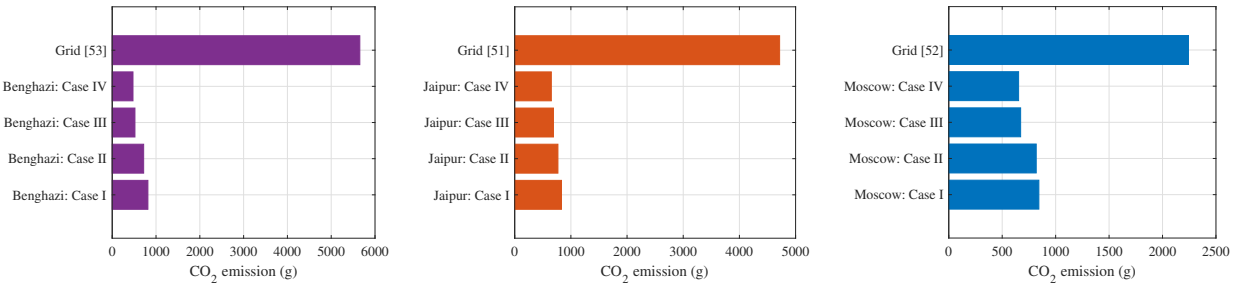

Fig. 14. CO_2 emission analysis for a) Benghazi, b) Jaipur, and c) Moscow at 40 Mbps for Case I, Case II, Case III, Case IV, and grid.

and the O&M cost is 2% of the asset cost [24]. The cost of the wind turbine is calculated as:

$$C_W = C_W^{asset} + C_W^{O\&M}, \tag{30}$$

The lifetime of PV panels and wind turbines is considered 20 yrs, therefore, no replacement for the PV panels and wind turbine is considered for analysis [24]. Table V shows the cost of batteries, PV panels and wind turbine. In terms of overall cost, the batteries are costlier compared to the PV panels, and the wind turbines are the cheapest. The cost of PV panel motor for rotation of the PV panel is considered to be \$0.1/W [51].

In Fig. 13, the cost analysis at different locations is shown. It can be observed from Fig. 13(a), that for case I, i.e., where the batteries are installed along with non-rotation PV panels has the highest cost for Benghazi followed by the case where batteries along with rotation PV panels. This is because the number of PV panels and batteries are reduced due to rotation of PV panels. For case III, where wind turbines are installed with PV panels without rotation the cost reduces from \$3112 to \$1276.25, which further reduces to \$1117.75 for case IV. Moreover, it can be seen that for case III and IV, the reduction in cost with respect to case I and II is significant because of the installation of wind turbines.

A similar trend can be observed in Figs. 13(b) and 13(c). It is evident that as the wind power in Benghazi is higher compared to Jaipur and Moscow, the reduction in the cost due to the installation of the wind turbine is greater for Benghazi compared to Jaipur and Moscow. A clear difference of \$1835.75 is observed at Benghazi for 20 Mbps throughput between the cost with and without wind turbine with fixed PV panel abd batteries, while that for Jaipur and Moscow is \$511.75 and \$947.75 for 20 Mbps throughput. Moreover, it can also be observed that the difference due to rotation of PV panels, i.e., case I and case II, and case III and case IV. decreases with the change in location from Benghazi to Moscow to Jaipur. This is because the wind power in Benghazi is high compared to Moscow and Jaipur.

C. Carbon footprint analysis

In this subsection, we evaluate the environmental impact of the energy resource allocation scheme in terms of CO_2 emissions. The CO_2 emissions for batteries, wind turbine and PV panels are mentioned in Table V. The batteries have the highest CO_2 emissions, followed by PV panels and wind turbines. The CO_2 emissions from the proposed solution are compared to the traditional grid power supply. The grid power can have a contribution from different energy sources such as thermal power, coal-based stations, gas-based stations, etc. According to the report by Central Electricity Authority, India on CO_2 baseline Database for the Indian power sector, 2018, the weighted average emission factor CO_2 emission for India is 0.82 t CO_2/MWh in 2017-18 [52]. The different components

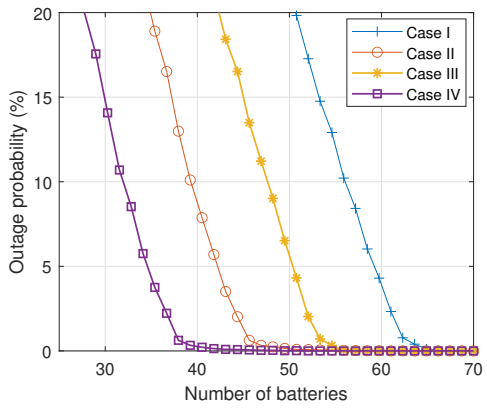

Fig. 15. Outage analysis for Jaipur at 40 Mbps throughput for Case I: Batteries with fixed PV panels, Case II: Batteries with fixed PV panels, Case III: Batteries with fixed PV panels and wind turbine, and Case IV: Batteries with rotational PV panels and wind turbine.

of CO_2 emission is mentioned in Table VI. Similarly, for Russia and Libya the CO_2 emissions are 0.39 t CO_2/MWh and 0.983 t CO_2/MWh, respectively [53], [54]. The environmental impact in terms of carbon dioxide (CO_2) emission for Benghazi, Jaipur, and Moscow is shown in Fig. 14. It can be seen that in the case of only grid power supply, the CO_2 emissions are the highest. For Benghazi at 40 Mbps, a CO_2 reduction of 96.8 g can be observed for case II compared to case I due to installation of rotational PV panels, and a reduction of 295.99 g due to installation of wind turbine along with fixed PV panels compared to case I. Similarly, for Jaipur, case IV has the least CO_2 emission of 702.81 g , while for case I the CO_2 emission of 841.98 g can be observed. For Moscow, a reduction of 50.08 g, 164.44 g, and 188.62 g can be observed for case II, III and IV compared to case I.

TABLE VI
WEIGHTED AVERAGE SPECIFIC CO_2 EMISSIONS FROM THE DIFFERENT FOSSIL FUEL STATIONS FOR INDIA IN 2017-18 [52]

Energy sources	CO_2 Emissions
Coal-based stations	0.97 t CO_2/MWh
Diesel-based stations	0.70 t CO_2/MWh
Gas-based station	0.45 t CO_2/MWh
Lignite based stations	1.36 t CO_2/MWh

TABLE VII
TRADE-OFF ANALYSIS BETWEEN ALLOCATION EFFICIENCY AND COST FOR JAIPUR AT 40 MBPS

	Case I	Case II	Case III	Case IV
Outage (in %)	10%			
No. of batteries	56	39	49	32
Cost (in $) (Assuming battery cost of $X)	$56X	$39X	$49X	$32X
Outage (in %)	5%			
No. of batteries	59	42	51	35
Cost (in $) (Assuming each battery cost $X)	$59X	$42X	$51X	$35X

Furthermore, a significant reduction of 91.61%, 86.17%, and 70.86% CO_2 emissions is evident for Benghazi, Jaipur and Moscow, respectively by using batteries along with rotational PV panels and wind turbine in place of traditional grid power supply.

D. Trade-off analysis between allocation efficiency and cost

In this subsection, we analyse the trade-off between allocation efficiency and cost, which is an important factor for the allocation of resources to power the ONU-AP. The allocation efficiency can be analysed as outage, i.e., the number of times the system is not able to fulfill the power the ONU-AP or number of times the battery level goes below the depth of discharge value [20]. The lower the outage higher is the allocation efficiency. In order to achieve lower outage, the number of batteries required by the ONU-AP will increase. As the cost of the battery might vary depending on the location, therefore, we have considered the cost of one battery as '$X'. From Fig. 15, it is evident that as the efficiency of energy resource allocation increases (or the outage decreases), the number of batteries (or cost of the system) also increases. Further, it is obvious from Table VII that for case I, as the allocation efficiency, i.e., outage increases from 5% to 10%, the cost decreases from $59X to $56X. Similarly, for case IV, a decrease in outage from 10% to 5% increases the cost by $3X. Further, it can also be observed from Fig. 15 that the cost of case II is lower compared to case III. This is because the solar power in Jaipur is high compared to wind power, as can be observed from Figs. 6 and 8(b).

Table VIII summarizes the environmental and cost impact of the energy resource allocation scheme. It can be seen for all the three locations, case IV where batteries are installed with wind turbines and rotational PV panels has the least cost and emits the lowest CO_2 emission. This is because case IV has the least number of PV panels and batteries required to power ONU-AP. Moreover, the cost comparison at Benghazi for 40 Mbps shows that a cost reduction of 48.43% is observed for case III compared to case I because of wind power supply. Similarly for case IV, a cost reduction of 53.81% is observed for Benghazi compared to case I because of wind and solar power profile. Furthermore, a CO_2 reduction of 11.84%, 36.25%, and 41.71% is observed at Benghazi for 40 Mbps throughput from case I to case II, III, and IV, respectively. While for Moscow cost reduces to 5.42%, 24.64%, 27.18% for case II, III, and IV compared to case I.

VIII. CONCLUSIONS

In this paper, we proposed a joint energy resource optimization framework to allocate energy resources to power ONU-AP. A two-step iterative algorithm is employed to calculate the energy resources required by ONU-AP for the off-grid scenario based on throughput profile and location of installation. Consequently, the joint energy resource allocation for different cases are analysed, namely, a) Case I: batteries with fixed PV panels, b) Case II: batteries with rotational PV panels, c) Case III: batteries with fixed PV panels and

TABLE VIII
COST AND ENVIRONMENTAL IMPACT ANALYSIS FOR 40 MBPS THROUGHPUT

	Cost Analysis($/W)				CO_2 emissions (g/W)			
Location	Case I	Case II	Case III	Case IV	Case I	Case II	Case III	Case IV
Benghazi	15.98	14.11	8.24	7.38	4.22	3.72	2.69	2.46
Jaipur	16.48	15.12	14.26	13.43	4.36	3.99	3.87	3.64
Moscow	16.96	16.04	12.78	12.35	4.50	4.24	3.65	3.52

wind turbines, and d) Case IV: batteries with rotational PV panels and wind turbines. It is interesting to note that for a location like Benghazi, the number of batteries reduce from 42 to 24 with the introduction of wind power supply with fixed PV panels, whereas a reduction of 20 batteries and 6 PV panels is observed at 60 Mbps throughput with the introduction of wind turbine and rotational PV panels. Moreover, in order to validate the accuracy of the algorithm, an analytical framework is derived. The good agreement between the results of analytical and iterative approach justifies the accuracy of the proposed framework. Furthermore, a socio-economic analysis is presented to analyse the impact of energy resource allocation on CO_2 emissions and the cost of the system. For Benghazi at 40 Mbps throughput, a reduction in cost of 11.62%, 48.42%, and 53.79% is observed for case II, III, and IV, respectively compared to case I, whereas, in terms of CO_2 emissions, a reduction of 11.89%, 36.33%, and 41.81% can be observed for case II, III and IV, respectively compared to case I. Moreover, the trade-off between energy resource allocation efficiency and cost is also analysed in the paper.

REFERENCES

[1] "Series G: Transmission systems and media, digital systems and networks, Gigabit-capable passive optical network (G-PON), G.987.3, ITU-T," Jan 2014.

[2] "Series G: Transmission coverage (TC) specifications-release2, 10-Gigabit-capable passive optical network (XG-PON), G.987.3, ITU-T," Jan 2014.

[3] "Series G: Transmission systems and media, digital systems and networks, 10-Gigabit-capable symmetric passive optical network (XGS-PON), G.9807.1, ITU-T," June 2016.

[4] "Series G: Transmission systems and media, digital systems and networks : 40-Gigabit-capable passive optical networks (NG-PON2): General requirements, G.989.1, ITU-T," March 2013.

[5] "IEEE 802.3ah-2004 - IEEE Standard for information technology– Local and metropolitan area networks– Part 3: CSMA/CD access method and physical layer specifications amendment: Media access control parameters, physical layers, and management parameters for subscriber access networks," September 2004.

[6] "IEEE 802.3av-2009 - IEEE Standard for information technology– Local and metropolitan area networks– Specific requirements– Part 3: CSMA/CD access method and physical layer specifications amendment 1: Physical layer specifications and management parameters for 10 Gb/s passive optical networks," September 2004.

[7] "IEEE 802.3 industry connections feasibility assessment for the next generation of EPON," March 2015.

[8] "IEEE Standard for Ethernet amendment 9: Physical layer specifications and management parameters for 25 Gb/s and 50 Gb/s passive optical networks," *IEEE Std 802.3ca-2020 (Amendment to IEEE Std 802.3-2018 as amended by IEEE 802.3cb-2018, IEEE 802.3bt-2018, IEEE 802.3cd-2018, IEEE 802.3cn-2019, IEEE 802.3cg-2019, IEEE 802.3cq-2020, IEEE 802.3cm-2020, and IEEE 802.3ch-2020)*, pp. 1–267, 2020.

[9] R. Kaur, A. Gupta, A. Srivastava, B. C. Chatterjee, A. Mitra, B. Ramamurthy, and V. A. Bohara, "Resource allocation and QoS guarantees for real world IP traffic in integrated XG-PON and IEEE802.11e EDCA networks," *IEEE Access*, vol. 8, pp. 124 883–124 893, 2020.

[10] A. Gupta, H. Goel, V. A. Bohara, and A. Srivastava, "Performance evaluation of integrated XG-PON and IEEE 802.11ac based EDCA networks," in *2020 IEEE International Conference on Advanced Networks and Telecommunications Systems (ANTS)*, 2020, pp. 1–6.

[11] A. Gupta, A. Srivastava, and V. A. Bohara, "Resource allocation in solar-powered FiWi networks," *IEEE Access*, vol. 8, pp. 198 691–198 705, 2020.

[12] H. Zhang, Y. Hu, R. Wang, Z. Li, P. Zhang, and R. Xu, "Energy efficient frame aggregation scheme in IoT over fiber-wireless networks," *IEEE Internet of Things Journal*, pp. 1–1, 2021.

[13] Z. Li, Q. Wang, and H. Zou, "QoE-aware video multicast mechanism in fiber-wireless access networks," *IEEE Access*, vol. 7, pp. 123 098–123 106, 2019.

[14] M. Lévesque and M. Maier, "Probabilistic availability quantification of PON and WiMAX based FiWi access networks for future smart grid applications," *IEEE Transactions on Communications*, vol. 62, no. 6, pp. 1958–1969, 2014.

[15] A. Mesodiakaki, P. Maniotis, M. Gatzianas, C. Vagionas, N. Pleros, and G. Kalfas, "A gated service MAC protocol for sub-ms latency 5G fiber-wireless MmWave C-RANs," *IEEE Transactions on Wireless Communications*, pp. 1–1, 2020.

[16] G. O. Pérez, A. Ebrahimzadeh, M. Maier, J. A. Hernández, D. L. López, and M. F. Veiga, "Decentralized coordination of converged tactile internet and MEC services in H-CRAN fiber wireless networks," *Journal of Lightwave Technology*, vol. 38, no. 18, pp. 4935–4947, 2020.

[17] A. Ebrahimzadeh and M. Maier, "Cooperative computation offloading in FiWi enhanced 4G HetNets using self-organizing MEC," *IEEE Transactions on Wireless Communications*, vol. 19, no. 7, pp. 4480–4493, 2020.

[18] D. P. Van, B. P. Rimal, M. Maier, and L. Valcarenghi, "ECO-FiWi: An energy conservation scheme for integrated fiber-wireless access networks," *IEEE Transactions on Wireless Communications*, vol. 15, no. 6, pp. 3979–3994, 2016.

[19] P. Han, L. Guo, Y. Liu, J. Hou, and X. Han, "Joint wireless and optical power states scheduling for green multi-radio fiber-wireless access network," *Journal of Lightwave Technology*, vol. 34, no. 11, pp. 2610–2623, 2016.

[20] V. Chamola, B. Krishnamachari, and B. Sikdar, "Green energy and delay aware downlink power control and user association for off-grid solar powered base stations," *IEEE Systems Journal*, vol. PP, pp. 1–12, 12 2016.

[21] V. Chamola, B. Sikdar, and B. Krishnamachari, "Delay aware resource management for grid energy savings in green cellular base stations with hybrid power supplies," *IEEE Transactions on Communications*, vol. PP, pp. 1–1, 11 2016.

[22] D. Benda, S. Sun, X. Chu, A. Buckley, and T. Q. S. Quek, "Optimal deployment of energy harvesters with anti-correlated energy generation at base stations," in *ICC 2020 - 2020 IEEE International Conference on Communications (ICC)*, 2020, pp. 1–6.

[23] R. Kaur, V. Krishnasamy, N. K. Kandasamy, and S. Kumar, "Discrete multiobjective grey wolf algorithm based optimal sizing and sensitivity analysis of PV-wind-battery system for rural telecom towers," *IEEE Systems Journal*, vol. 14, no. 1, pp. 729–737, 2020.

[24] R. Atia and N. Yamada, "Sizing and analysis of renewable energy and battery systems in residential microgrids," *IEEE Transactions on Smart Grid*, vol. 7, no. 3, pp. 1204–1213, 2016.

[25] J. Wang, H. Zhong, W. Tang, R. Rajagopal, Q. Xia, and C. Kang, "Tri-level expansion planning for transmission networks and distributed

energy resources considering transmission cost allocation," *IEEE Transactions on Sustainable Energy*, vol. 9, no. 4, pp. 1844–1856, 2018.
[26] D. Alder, A. Khodaei, and W. David Gao, "Standard measurement of carbon footprints," in *2016 North American Power Symposium (NAPS)*, 2016, pp. 1–5.
[27] "Grid-tied solar vs. off-grid solar: What are the pros and cons of both?" [Online]. Available: https://www.paradisesolarenergy.com/blog/grid-tied-solar-vs-off-grid-solar-what-are-the-pros-and-cons-of-both
[28] "On-grid solar power systems vs off-grid solar power systems: Their applications advantages." [Online]. Available: https://economictimes.indiatimes.com/small-biz/productline/power-generation/on-grid-solar-power-systems-vs-off-grid-solar-power-systems-their-//applications-advantages/articleshow/69200840.cms?utm_source=contentofinterest&utm_medium=text&utm_campaign=cppst
[29] Z. Gu, H. Lu, and Z. Zhu, "On throughput optimization and bound analysis in cache-enabled fiber-wireless networks," *IEEE Transactions on Vehicular Technology*, vol. 69, no. 8, pp. 9068–9082, 2020.
[30] "Whether GPON will replace EPON in the future," 2020. [Online]. Available: https://cdatatec.com/whether-gpon-will-replace-epon-future/
[31] "Global passive optical network (PON) equipment industry," 2021. [Online]. Available: https://www.reportlinker.com/p05817750/Global-Passive-Optical-Network-PON-Equipment-Industry.html?utm$_$source=GNW
[32] N. E, X. Chu, W. Guo, and J. Zhang, "User data traffic analysis for 3G cellular networks," 08 2013, pp. 468–472.
[33] M. Theologou, M. Louta, G. Papadimitriou, and P. Sarigiannidis, "Analysing the optical network unit power consumption in the 10 GB-capable passive optical network systems," *IET Networks*, vol. 5, 02 2016.
[34] L. Xue, L. Yi, H. Ji, P. Li, and W. Hu, "Symmetric 100-Gb/s TWDM-PON in O-band based on 10G-class optical devices enabled by dispersion-supported equalization," *Journal of Lightwave Technology*, vol. 36, no. 2, pp. 580–586, 2018.
[35] C. B. Gaur, V. Gordienko, F. Bessin, and N. J. Doran, "Dual-band amplification of downstream L-band and upstream C-band signals by FOPA in extended reach PON," in *2020 European Conference on Optical Communications (ECOC)*, 2020, pp. 1–4.
[36] A. Garcia-Saavedra, P. Serrano, A. Banchs, and G. Bianchi, "Energy consumption anatomy of 802.11 devices and its implication on modeling and design," in *Proceedings of the 8th International Conference on Emerging Networking Experiments and Technologies*, ser. CoNEXT '12. New York, NY, USA: Association for Computing Machinery, 2012, p. 169–180. [Online]. Available: https://doi.org/10.1145/2413176.2413197
[37] "Push it to the limit! Understand Wi-Fi's breaking point to design better WLANs," 2015. [Online]. Available: https://blogs.arubanetworks.com/industries/pushittothelimitunderstandwifisbreakingpointtodesignbetterwlans/
[38] "NREL Renewable Resource Data Center," 2018. [Online]. Available: https://www.nrel.gov/grid/solar-resource/renewable-resource-data.html
[39] "Climate.OneBuilding.Org." [Online]. Available: http://climate.onebuilding.org/default.html
[40] A. A. Smirnov, A. G. Vozmilov, and P. A. Romanov, "Comparison of discrete sun tracking methods for photovoltaic panels," in *2019 International Conference on Industrial Engineering, Applications and Manufacturing (ICIEAM)*, 2019, pp. 1–5.
[41] "Global wind atlas." [Online]. Available: https://globalwindatlas.info/
[42] J. Ouyang, M. Li, Z. Zhang, and T. Tang, "Multi-timescale active and reactive power-coordinated control of large-scale wind integrated power system for severe wind speed fluctuation," *IEEE Access*, vol. 7, pp. 51 201–51 210, 2019.
[43] E. . R. B. . S. D. Büngeler, Johannes Cattaneo, "Advantages in energy efficiency of flooded lead-acid batteries when using partial state of charge operation," *Journal of Power Sources*, vol. 5, pp. 53–58, 01 2018.
[44] "IEEE guide for optimizing the performance and life of lead-acid batteries in remote hybrid power systems," *IEEE Std 1561-2019 (Revision of IEEE Std 1561-2007)*, pp. 1–34, 2019.
[45] P. Gurram, H. Kwon, Z. Peng, and W. Yin, "Optimal sparse kernel learning for hyperspectral anomaly detection," in *2013 5th Workshop on Hyperspectral Image and Signal Processing: Evolution in Remote Sensing (WHISPERS)*, 2013, pp. 1–4.
[46] "Prove linear programming is a special case of quadratic programming." [Online]. Available: https://math.stackexchange.com/questions/3881511/prove-linear-programming-is-a-special-case-of-quadratic-programming
[47] "AMP Chapter-13." [Online]. Available: http://web.mit.edu/15.053/www/AMP-Chapter-13.pdf
[48] O. Esrafilian and D. Gesbert, "Simultaneous user association and placement in multi-UAV enabled wireless networks," in *WSA 2018; 22nd International ITG Workshop on Smart Antennas*, 2018, pp. 1–5.
[49] Hi Link HLK 5M12 12V/5W Switch Power Supply Module. [Online]. Available: https://robu.in/product/hlk-5m12-12v-5w-switch-power-supply-module/?gclid=CjwKCAjwxuuCBhATEiwAIIIz0ThdavQEYruvk7H3S55NoOYa5Dwk2\0acFmXX0p-2eNCpYwBYPLMYjRoCYvEQAvD_BwE
[50] Solar India 5 Watt 6 V Polycrystalline Solar Panel SSI5 Watt. [Online]. Available: https://www.industrybuying.com/solar-panels-solar-india-SO.PO.1624861/?utm_source=Google&utm_medium=PLA&utm_campaign=PLA_New_Solar&gclid=CjwKCAjwxuuCBhATEiwAIIIz0cM4Smo1XsVvxLgq-dtdnkuTDZu_5hTLsX3IlJUvku4eVgdFvihZTRoC5ewQAvD_BwE
[51] Advantages and disadvantages of a solar tracker system. [Online]. Available: https://www.solarpowerworldonline.com/2016/05/advantages-disadvantages-solar-tracker-system/
[52] "CO_2 baseline database for the Indian power sector," 2018. [Online]. Available: https://cea.nic.in/wp-content/uploads/baseline/2020/07/user_guide_ver14.pdf
[53] "Brown to green: The G20 transition to a low-carbon economy," 2017. [Online]. Available: https://www.climate-transparency.org/wp-content/uploads/2017/07/B2G2017-Russia.pdf
[54] Y. Nassar, M. Salem, K. Iessa, A. Mohamed, A. Ibraheem, and M.F. Khaled, "Estimation of CO_2 emission factor for the energy industry sector in Libya: a case study," *Environment, Development and Sustainability*, 2021.